METEOR: Assessment of Vulnerability Uncertainty

Report Number: M5.3/P

8 April 2020

UK SPACE AGENCY

Contributors:
Nicole Paul
Vitor Silva
Ramesh Guragain
Sharad Wagle
Surya Narayan Shrestha

British Geological Survey
Expert | Impartial | Innovativ

FATHOM

GEM
GLOBAL EARTHQUAKE MODEL
working together to assess risk

Oxford Policy Management

HOT

ImageCat

NSET
Earthquake Safe Communities in Nep

METEOR Assessment of Vulnerability Uncertainty

UK SPACE AGENCY

Document Verification

Project	METEOR: Modelling Exposure Through Earth Observation Routines
Report Title	METEOR Outline of Educational Material and Tutorial Development
Related Milestone	M5.3
Reference as	Paul, N., Silva, V., Guragain, R., Wagle, S. and Shrestha, S. (2020) METEOR Assessment of vulnerability uncertainty. Report M5.3/P
Release Type	Public / ~~Confidential~~ / ~~Confidential with Embargo Period~~

Prepared by: Contributors		
Name(s): Nicole Paul Vitor Silva	Signature(s):	Date(s): 8 April 2020
Approved by: Project Manager		
Name: Kay Smith	Signature:	Date: 7 May 2020
Approved by: UKSA IPP Project Officer		
Name:	Signature:	Date:

Date	Version	Alterations	Editor

Abbreviations

Acronym	Full Text Description
BGS	British Geological Survey: An organisation providing expert advice in all areas of geoscience to the UK government and internationally
DMD	Disaster Management Department: Prime Minister's Office of Tanzania focused on disaster risk
DRM	Disaster Risk Management
DS	Damage State
EDP	Engineering Demand Parameters
EO	Earth Observation
FATHOM	Provides innovative flood modelling and analytics, based on extensive flood risk research
GCRF	Global Challenges Research Fund
GEM	Global Earthquake Model: Non-profit organisation focused on the pursuit of earthquake resilience worldwide
HOT	Humanitarian OpenStreetMap Team: A global non-profit organisation the uses collaborative technology to create OSM maps for areas affected by disasters
ImageCat	International risk management innovation company supporting the global risk and catastrophe management needs of the insurance industry, governments and NGOs
IPP	International Partnership Programme
IM	Intensity Measure
METEOR	Modelling Exposure Through Earth Observation Routines
NSET	National Society for Earthquake Technology: Non-governmental organisation working on reducing earthquake risk in Nepal and abroad
ODA	Official Development Assistance
OPM	Oxford Policy Management: Organisation focused on sustainable project design

	and implementation for reducing social and economic disadvantage in low-income countries
PDC	Pyroclastic Density Current
PGA	Peak Ground Acceleration
SDOF	Single Degree Of Freedom
SRSS	Square Root of the Sum of the Squares
UKSA	United Kingdom Space Agency
WP	Work Package

METEOR Assessment of Vulnerability Uncertainty

UK SPACE AGENCY

Contents

Figures

Tables

1. METEOR Project Introduction

1.1. Project Summary

Table 1: METEOR Project summary

Project Title	Modelling Exposure Through Earth Observation Routines (METEOR): EO-based Exposure, Nepal and Tanzania
Starting Date	08/02/2018
Duration	36 months
Partners	UK Partners: The British Geological Survey (BGS) (Lead), Oxford Policy Management Limited (OPM), SSBN Limited (Fathom) International Partners: The Disaster Management Department, Office of the Prime Minister – Tanzania (DMD), The Global Earthquake Model (GEM) Foundation, The Humanitarian OpenStreetMap Team (HOT), ImageCat, National Society for Earthquake Technology (NSET) – Nepal
Target Countries	Nepal and Tanzania for "level 2" results and all 47 Least Developed ODA countries for "level 1" data
IPP Project	IPPC2_07_BGS_METEOR

1.2. Project Overview

At present, there is a poor understanding of population exposure in some Official Development Assistance (ODA) countries, which causes major challenges when making Disaster Risk Management decisions. Modelling Exposure Through Earth Observation Routines (METEOR) takes a step-change in the application of Earth Observation exposure data by developing and delivering more accurate levels of population exposure to natural hazards. Providing new consistent data to governments, town planners and insurance providers will promote welfare and economic development in these countries and better enable them to respond to the hazards when they do occur.

METEOR is funded through the second iteration of the UK Space Agency's (UKSA) International Partnership Programme (IPP), funded through the Global Challenges Research Fund (GCRF), which uses space expertise to deliver innovative solutions to real world problems across the globe. The funding helps to build sustainable development while building effective partnerships that can lead to growth opportunities for British companies.

1.3. Project Objectives

METEOR aims to formulate an innovative methodology of creating exposure data through the use of EO-based imagery to identify development patterns throughout a country. Stratified sampling technique harnessing traditional land use interpretation methods modified to characterise building patterns can be combined with EO and in-field building characteristics to capture the distribution of building types. These protocols and standards will be developed for broad application to ODA countries and will be tested and validated for both Nepal and Tanzania to assure they are fit-for-purpose.

Detailed building data collected on the ground for the cities of Kathmandu (Nepal) and Dar es Salaam (Tanzania) will be used to compare and validate the EO generated exposure datasets. Objectives of the project look to: deliver exposure data for 47 of the least developed ODA countries, including Nepal and Tanzania; create hazard footprints for the specific countries; create open protocol; to develop critical exposure information from EO data; and capacity-building of local decision makers to apply data and assess hazard exposure. The eight work packages (WP) that make up the METEOR project are outlined below in section 1.4.

1.4. Work Packages

Outlined below are the eight work packages that make up the METEOR project, which are led by various partners. Table 2 provides an overview of the work packages together with a brief description of what each of the work packages cover.

Table 2: Overview of METEOR work packages

Work Package	Title	Lead	Overview
WP.1	Project Management	BGS	Project management, meetings with UKSA, quarterly reporting and the provision of feedback on project deliverables and direction across primary stakeholders.
WP.2	Monitoring and Evaluation	OPM	Monitoring and evaluation of the project and its impact, using a theory of change approach to assess whether the associated activities are leading to the desired outcome.
WP.3	EO Data for Exposure Development	ImageCat	EO-based data for exposure development, methods and protocols of segmenting/classifying building patterns for stratified sampling of building characteristics.
WP.4	Inputs and Validation	HOT	Collect exposure data in Kathmandu and Dar es Salaam to help validate and calibrate the data derived from the classification of building patterns from EO-based imagery.

WP.5	Vulnerability and Uncertainty	GEM	Investigate how assumptions, limitations, scale and accuracy of exposure data, as well as decisions in data development process lead to modelled uncertainty.
WP.6	Multiple Hazard Impact	BGS	Multiple hazard impacts on exposure and how they may be addressed in disaster risk management by a range of stakeholders.
WP.7	Knowledge Sharing	GEM	Disseminate to the wider space and development sectors through dedicated web-portals and use of the Challenge Fund open databases.
WP.8	Sustainability and Capacity-Building	ImageCat	Sustainability and capacity-building, with the launch of the databases for Nepal and Tanzania while working with in-country experts.

2. Introduction to work package

Uncertainty is fundamental to disaster risk assessment, both from the inherent randomness of natural phenomena (e.g., depth of rainfall in a 24-hour storm) and due to our incomplete scientific knowledge of the phenomena (e.g., lack of sufficient damage data, appropriateness of a given mathematical model). These areas of uncertainty are referred to as aleatory variability and epistemic uncertainty, respectively. Lack of consideration of these sources of uncertainty in disaster risk assessment can lead to erroneous decision making. Therefore, it is essential to consider different aspects of uncertainty in the various components that compose a disaster risk assessment, and propagate those through the entire process to get a full view of the range of possible outcomes. The incorporation of all sources of uncertainty in risk assessment is a fundamental goal of the METEOR project.

This report focuses on four key areas of uncertainty related to vulnerability and exposure models. These areas include variabilities in the hazard input, building capacity, damage threshold and loss model. While this report evaluates the impact of these uncertainties on vulnerability models, a forthcoming report (M5.4) will propagate the uncertainties to both urban and regional risk assessments. Moreover, additional information about the consideration of aleatory variability and epistemic uncertainty in the hazard and exposure counterparts can be found in Deliverables M3.2 (Huyck, et al., 2019) and M6.1 (Winson, et. al., 2019).

3. Natural hazards vulnerability models and uncertainty

3.1. Fragility and vulnerability models

Fragility and vulnerability models are a fundamental component of natural hazard risk assessment. Fragility functions quantify the probability of exceeding a set of damage states (e.g. slight damage, moderate damage) for a given hazard intensity value. Those damage states can then be related to a loss ratio value or distribution. Vulnerability functions combine these two aspects to directly quantify the average damage or loss ratio for a given hazard intensity value. Generic examples of these models are shown in Figure 1.

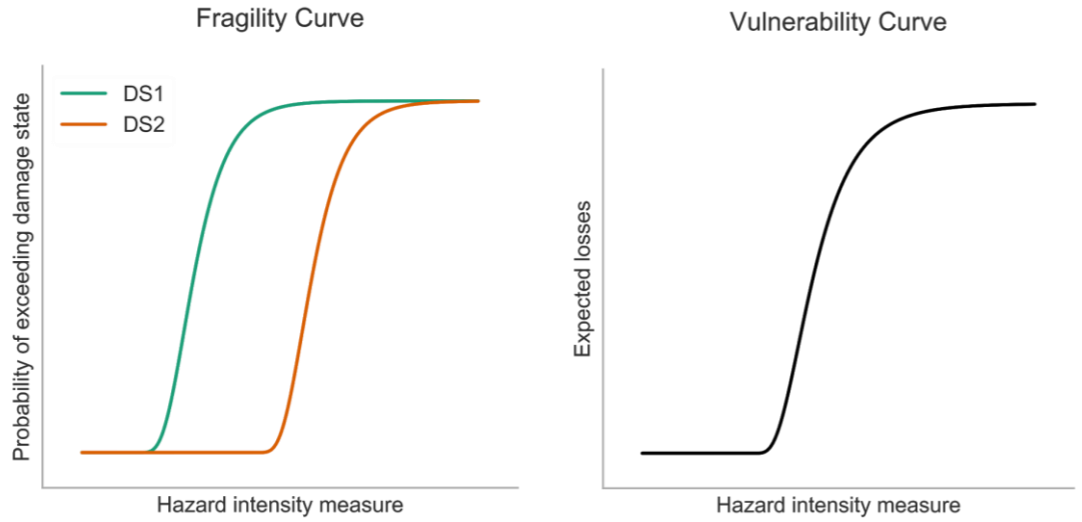

Figure 1: Graphical representation of a fragility curve for two hypothetical damages states, DS (left) and vulnerability curve (right)

Fragility and vulnerability models can be derived using empirical data, analytical methods, expert judgment, or hybrid methods. A derived fragility or vulnerability function should ideally be developed specifically for the exposure in the region of interest (e.g., considering construction materials or practices local to the area of interest). The use of empirical data is ideal, but there tends to be a lack of sufficient data, particularly for larger intensity natural hazard events that are rarer. Analytical methods can address the problem of insufficient empirical data, but entail several simplifying assumptions that require a balance between accuracy and computational space or time demands. Additionally, the complexity or number of unique fragility or vulnerability functions must be bounded by the resolution of exposure data, and/or require development of a mapping scheme to go from lower resolution exposure data to higher resolution vulnerability models.

This report explores the propagation of uncertainty in assumptions inherent to fragility or vulnerability function derivation using analytical methods. The analytical method of fragility derivation was chosen for this study because it can explicitly account for sources of uncertainty. These uncertainties are broadly categorised into hazard representation, building capacity variability, damage measure criteria definitions and loss ratio variability.

3.2. Earthquakes

Vulnerability modelling of buildings for earthquake ground shaking has been a wide area of research for decades, and thus there is comparatively more published research on this topic as compared with the other considered hazards. Analytical seismic fragility and vulnerability models can be derived using either static or dynamic methods, but typically require an estimate of seismic ground shaking input (e.g. response spectra), simplification of a building into limited dynamic response values (e.g. equivalent single degree of freedom, or SDOF, parameters) and establishment of demand-based damage criteria (e.g. drift thresholds).

As with other natural hazards, quantification of seismic hazard for the purpose of risk assessment often relies on a singular parameter or metric. The peak ground acceleration (PGA) is the most commonly used hazard metric for earthquakes. However, the spectral acceleration at the fundamental period of the structure, $S_a(T)$, has a higher correlation with damage than PGA and several other hazard metrics (Elenas, et al., 2001). In either case, other aspects of ground motion (e.g., duration, spectral acceleration at other periods, site soil effects) can induce varying responses in buildings, and therefore cause different levels of damage (Sousa, et al., 2015; Chandramohan, et al., 2016; Gehl, et al., 2013). The variability of response tends to increase with increasing damage level, as the dynamic properties of the building vary with damage. For this reason, national building codes (e.g., ASCE7 in the United States[1]) often prescribe a minimum number of ground motion records to be considered in the dynamic analysis of structures both for design and safety assessment.

Similarly, there are many different parameters associated with the response of a structure, often referred to as "engineering demand parameters", or *EDP*s. The *EDP* most commonly used for earthquake response of buildings is related to the displacement, as it tends to be the most correlated with damage. However, other aspects of response can also contribute to damage (e.g., floor accelerations). Damage state thresholds similarly often use displacement-based criteria, but have an inherent randomness (e.g., buildings of a given typology could collapse at a range of different displacement values). These damage states then must be translated into losses, which have a similar variability to all the other considered hazards.

3.3. Landslides

Fragility and vulnerability functions for landslides have been published, using a range of metrics to quantify the hazard input. This is partially due to the fact that landslides can be triggered in different manners, such as from an earthquake or from heavy rainfall. Some of the used hazard metrics include peak ground acceleration, permanent ground deformation and equivalent cumulative displacement. Similar to other dynamic natural hazards, there are a variety of characteristics or mechanisms of a landslide that could result in varying damage to structures, which cannot be easily quantified as a single metric. Some of these factors include speed of the landslide, soil/rock properties and landslide geometry.

The representation of physical vulnerability of buildings to landslides typically involves an estimate of global building strength, based on construction material and quality. Although some analytical fragility or

[1] Available online at: https://www.asce.org/structural-engineering/asce-7-and-sei-standards/

vulnerability functions for landslides exist (Fotopoulou, et al., 2013; Haugen, et al., 2008), expert elicitation is more commonly used to assess physical vulnerability of landslides due to an inability of some of these analytical models to successfully simulate past observations of damage (Guillard-Gonçalves, et al., 2016; Singh, et al., 2019). Common indicators of physical vulnerability of buildings to landslides include: height of lowest opening, foundation type, roof material, basement presence, state of maintenance, number of floors, and construction material (Dabbeek, et al., 2020; Singh, et al., 2019). Since there are relatively few studies that involve analytical derivation of fragility or vulnerability models, a direct assessment of uncertainty propagation for landslides is challenging. Additionally, expert elicitation methods tend to provide qualitative (as opposed to quantitative) outputs, which increases the challenge.

3.4. Volcanoes

Fragility and vulnerability functions are less prevalent for volcanoes than for many other natural hazards, and are an area of active scientific research and development. Published functions often use tephra (ashfall) thickness or load to quantify the hazard input and simplify the building based on its roof material and pitch (Pomonis, et al., 1999; Spence, et al., 2008; Zuccaro, et al., 2008; Jenkins, et al., 2014). Tephra fall is an appealing metric for risk assessment, given it is one of the most widespread and frequent volcanic hazards, affecting large areas with impacts at relatively low thicknesses (Blong, et al., 2017; Magill, et al., 2005). Although tephra thickness or load is commonly used as the metric to quantify building damage from volcanic hazards, there are many additional metrics that could result in building damage from a given scenario, including: lahar, lava flow, debris and pyroclastic density currents (Sparks, et al., 2013; Wilson, et al., 2014). Pyroclastic density currents (PDCs) and lava flow can produce more intense damage, but tend to only affect buildings in the immediate vicinity of the volcano.

Analytical estimations of tephra fall require assumptions around meteorological conditions (e.g., wind speed and direction, wet or dry) and ash dispersal, thereby introducing uncertainty. Some of these parameters could directly affect vulnerability models (e.g., wet versus dry tephra could result in different damage levels at the same thickness value), whereas other aspects would primarily affect the hazard quantification and therefore the risk assessment. Additionally, buildings of similar roof material and pitch can have varying strength, connection details, and geometry, thereby resulting in varying response to equivalent tephra loads. In contrast to landslides and earthquakes, analytical estimates of building damage due to tephra fall tend to be static (i.e., not dynamic), which implies less variability with respect to building response given a hazard intensity level. Similar to other discussed hazards, damage state thresholds and associated loss ratios must also be established. Roof collapse is commonly considered as the damage state, which might have varying associated loss ratios based on factors such as the building height (e.g., roof collapse of a single-story structure may be considered a complete loss, whereas a taller structure may consider it as a partial loss).

3.5. Flooding

Several flood fragility and vulnerability functions have been published over the years (Pregnolato, et al., 2015), typically using flood depth to quantify the hazard input and directly relating that to a damage or loss ratio. Unlike the other considered natural hazards, derivation of flood vulnerability models tends to have less emphasis on building analysis or characteristics such as strength or dynamic properties.

Flood hazard models are reliant on a variety of data sources and types, such as digital elevations, boundary conditions, flow rates, and effective roughness parameters. Some studies have shown that even small variations in inputs like the digital elevation model can lead to large variance in the estimated inundation depths (Zerger, et al., 2002). Additionally, there is inherent randomness in factors such as storm duration and rainfall depth. On top of that, estimates of these parameters are subject to a changing baseline due to climate change, which can limit the applicability of the available historic data (Kundzewicz, et al., 2014).

In addition to flood depth, alternate hazard metrics such as duration, velocity, or surge can also incur damage and therefore loss to exposed buildings. Although there is likely less variance in building response to equivalent flood depths than the other, more dynamic natural hazards, there may still be some differences building to building with the existence of flood defence systems and the existence of below-grade floors or contents.

4. Case study of uncertainty in vulnerability models

4.1. Methodology

The propagation of uncertainty was performed for masonry buildings in Nepal considering earthquake ground shaking. However, the framework is generic and many takeaways equally pertain to the other natural hazards, locations and building typologies. The four broad categories of uncertainty that were considered are summarised in Table 3.

Table 3: Description of four sources of uncertainty investigated within this work package

Category	Description
Hazard input	Although singular hazard metrics are often chosen for ease of computation, there are many other factors that could influence building response. This is particularly true for dynamic hazards, such as earthquakes and landslides. This area of uncertainty is explored by using different hazard inputs with equivalent values at a given intensity level, versus considering multiple hazard inputs across a range of intensity levels.
Building-to-building	Fragility or vulnerability curves require an estimate of building capacity or strength to the hazard of interest, but robust assessment of capacity typically requires more detailed information that is available in large-scale studies. However, it is not common practice to directly consider uncertainty in these estimates. Randomly sampled capacity curves were generated based on the mean capacity curves of the considered building typologies to assess this area of variability.
Damage state threshold	Fragility curves tend to differentiate between varying degrees of damage (e.g., slight, moderate, extensive, complete). However, this requires the establishment of a damage threshold, which in reality has an inherent degree

	of randomness. A probabilistic distribution for this parameter was considered on this threshold to assess the implications of this uncertainty.
Loss ratio	Damage states indicate a broad state of damage (e.g., slight, moderate, extensive, complete), but the proportion of loss associated with that state is inherently random. This study investigated the use of expected loss ratios at each damage state, versus modelling a Beta distribution for each damage state.

In this report, the impact on the resulting vulnerability of each building typology was evaluated through several different manners, including:

- Distribution of resulting fragility or vulnerability models
- Distribution of average annual losses, or expected loss in a given timeframe
- Coefficient of variation of losses per intensity level

The next deliverable will instead focus on the impact of these uncertainties on disaster risk assessments at both the urban and national level. A visual representation of the logic tree to represent each of these cases is shown in Figure 2.

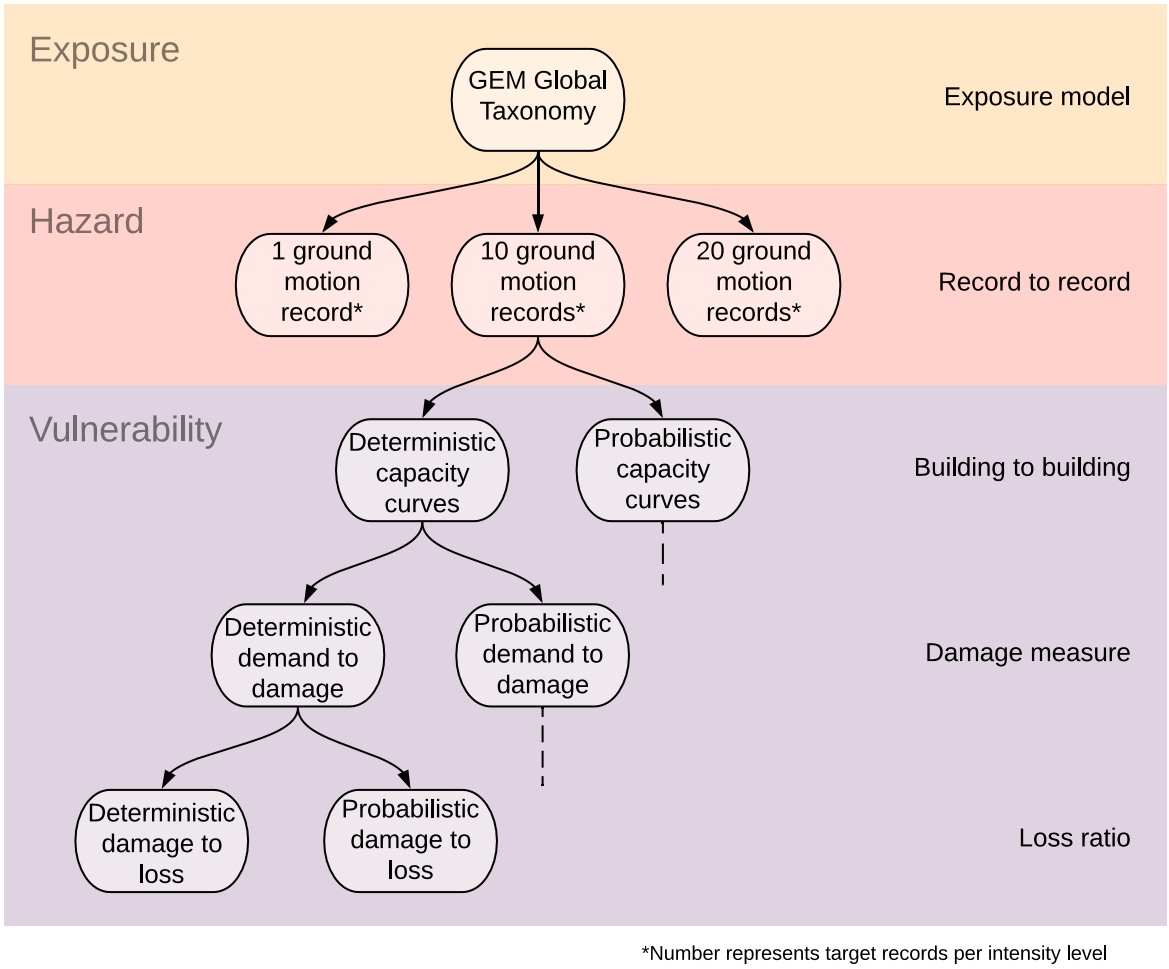

Figure 2: Logic tree that describes the branches analysed to study each source of uncertainty

For this study, unreinforced masonry typologies common to Nepal were investigated. The typologies considered are summarised in Table 4, with their associated mean capacity curves shown in Figure 7.

Table 4: Building typologies investigated for uncertainty propagation study

GEM Taxonomy	Material	Lateral system	Stories
MUR/LWAL/DNO/H:1	Unreinforced masonry, unknown units*	Wall, no ductility	1
MUR/LWAL/DNO/H:2			2
MUR/LWAL/DNO/H:3			3
MUR/LWAL/DNO/HBET:4-5			4-5
MUR+ADO/LWAL/DNO/H:1	Unreinforced masonry, adobe blocks		1
MUR+ADO/LWAL/DNO/H:2			2
MUR+ST/LWAL/DNO/H:1	Unreinforced masonry, unknown stone		1
MUR+ST/LWAL/DNO/H:2			2
MUR+ST/LWAL/DNO/H:3			3

**Unknown masonry units could include any of the following types: rubble stone, fired clay (hollow or solid), concrete, stone, or adobe.*

4.2. Hazard input variability

The characterisation of natural hazards often relies on the selection of one or more intensity measures (*IM*), which reduces the complexity of the phenomena into quantifiable measures. Ideally, the selected IM will correlate strongly with damage or losses and is practical to estimate.

Although single *IM*s are commonly used, other characteristics of the hazard at a given intensity level may influence the degree of damage, particularly for dynamic hazards (e.g., landslides, earthquakes) once a structure has gone into the inelastic region of response (i.e. once damage initiates). This variability of response is considered as "hazard input variability" in this report, but may be referred to as other names within the hazard-specific context (e.g. "record-to-record variability" for earthquakes). Common *IM*s for each of the considered hazards are presented in Table 5, with some commentary on other metrics that could induce variability in structural response and therefore fragility or vulnerability models. An example of two potential hazard inputs with equivalent *IM* values is shown in Figure 3 for the earthquake hazard.

Table 5: Summary of hazard input factors that contribute to uncertainty in vulnerability estimates

Hazard	Intensity measure*	Other hazard factors that contribute to damage variability
Earthquake	Peak ground acceleration, spectral acceleration at fundamental period	Spectral shape, duration of strong shaking, site-specific soil conditions, topographical conditions
Landslide	Peak ground acceleration, equivalent cumulative displacement	Mechanism of landslide, speed of landslide
Flood	Flood depth	Flood velocity, flood duration, storm surge
Volcano	Tephra thickness	Meteorological conditions

**The most commonly used intensity measures are presented for clarity*

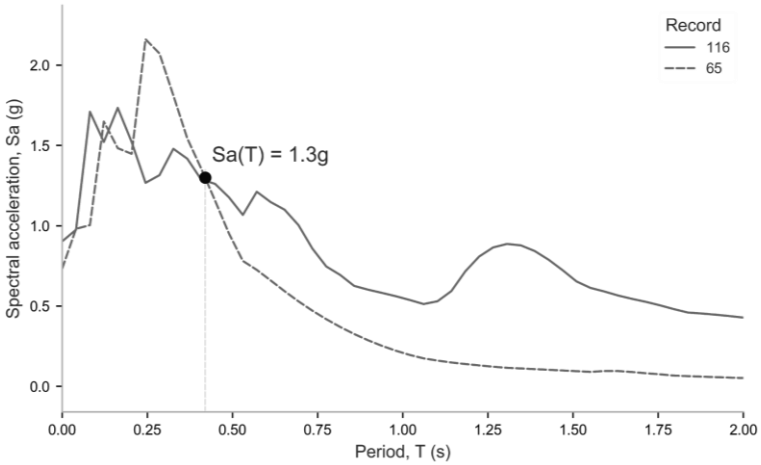

Figure 3: Comparison of two alternate ground motion records with comparable values of spectral acceleration at the period of interest (T=0.42)

Since earthquakes are dynamic hazards, the individual ground motion record associated with an event can have a significant influence on the behaviour of the structure and its resulting damage. Once in the inelastic region of response (i.e. once damage initiates), additional modes contribute to the behaviour of the structure, such that multiple ground motions with the same *IM* value (e.g., $S_a(T_1)$) can lead to varying peak response values and damage. As a result, structures evaluated with relatively few ground motion records (often amplitude-scaled to cover different intensity levels) can exhibit biased nonlinear response behaviour. This is demonstrated by the varying fragility and vulnerability curves.

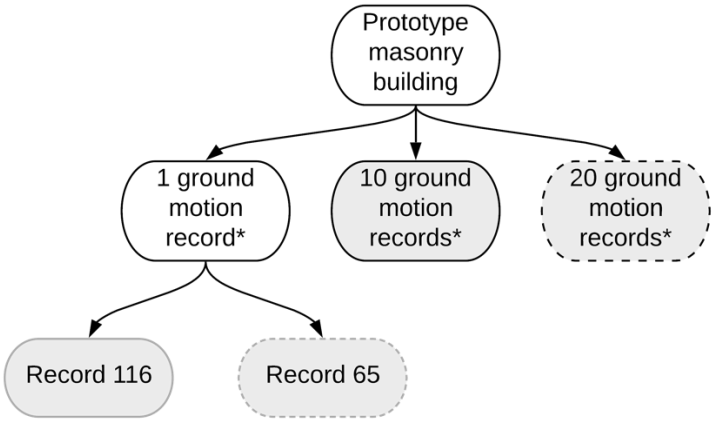

Figure 4: Logic tree describing different cases (endpoints filled in grey) studied to demonstrate hazard input variability

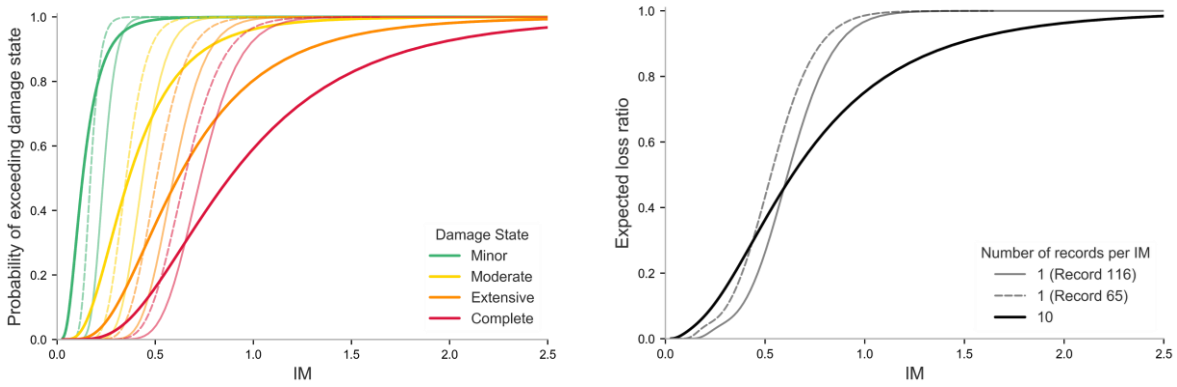

Figure 5: Comparison of resulting fragility curves (left) and vulnerability curves (right) from two alternate ground motion records versus 10 ground motion records per IM for building typology with T=0.42s, MUR+ST/LWAL+DNO/H:3

The resulting fragility and vulnerability curves in Figure 5 show the impact of considering multiple sets of hazard inputs at each intensity measure level. Limiting the analysis to 1 record per intensity measure level gives the illusion of increased certainty (as evidenced by the steeper slope), but the range of the distribution is biased and could sit anywhere along the range of the distribution seen using 10 records per intensity measure level. Although the consideration of 10 (versus just 1) records at each intensity level has a dramatic effect on the resulting fragility and vulnerability curves, the same degree of difference does not hold for consideration of 20 (versus just 10) records at each intensity level. This analysis is shown in Figure 6, where it can be seen that the curves with 20 records almost completely overlap with the curves with 10 records. This implies that considering 10 records per intensity level should be sufficient for fragility or vulnerability derivation.

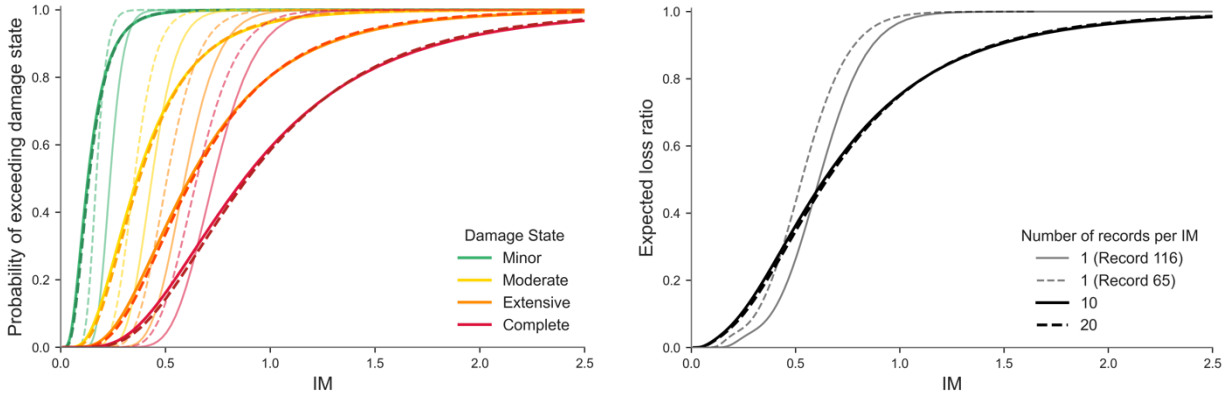

Figure 6: Comparison of resulting fragility curves (left) and vulnerability curves (right) from two alternate ground motion records versus 10 and 20 ground motion records per IM for building typology with T=0.42s, MUR+ST/LWAL+DNO/H:3

4.3. Building-to-building variability

Disaster risk assessment typically relies on the identification of a finite number of building typologies or archetypes, which relate the exposure data to a fragility or vulnerability model. These building typologies and their associated fragility or vulnerability curves are intended to represent a group of buildings with similar features, but not intended to represent individual buildings or assets. Building or asset-specific fragility and vulnerability models would require high resolution exposure data, which typically is not available nor practically developed for large-scale studies. As such, it is anticipated there will be some variability in damage or losses due to the building-to-building variability within a given building archetype. This could be due to varying construction quality, presence of structural irregularities, or a host of other differences within the building stock. For low-strength masonry buildings, the seismic performance can be particularly sensitive to the number of stories, therefore the taxonomy used herein differentiates between building heights as seen in Figure 7 and Table 6.

Commonly, an estimate of building strength or capacity is required, usually using construction age or material type as a proxy to estimate that value. Example capacity curves estimates for the considered unreinforced masonry buildings in Nepal are shown in Figure 7 and Table 6. These refer to the 'best estimate' of capacity of these building typologies, however there is some inherent randomness as described earlier. For masonry buildings and their seismic performance, variations in wall thickness and mortar strength can be particularly influential to the seismic displacement and acceleration, respectively.

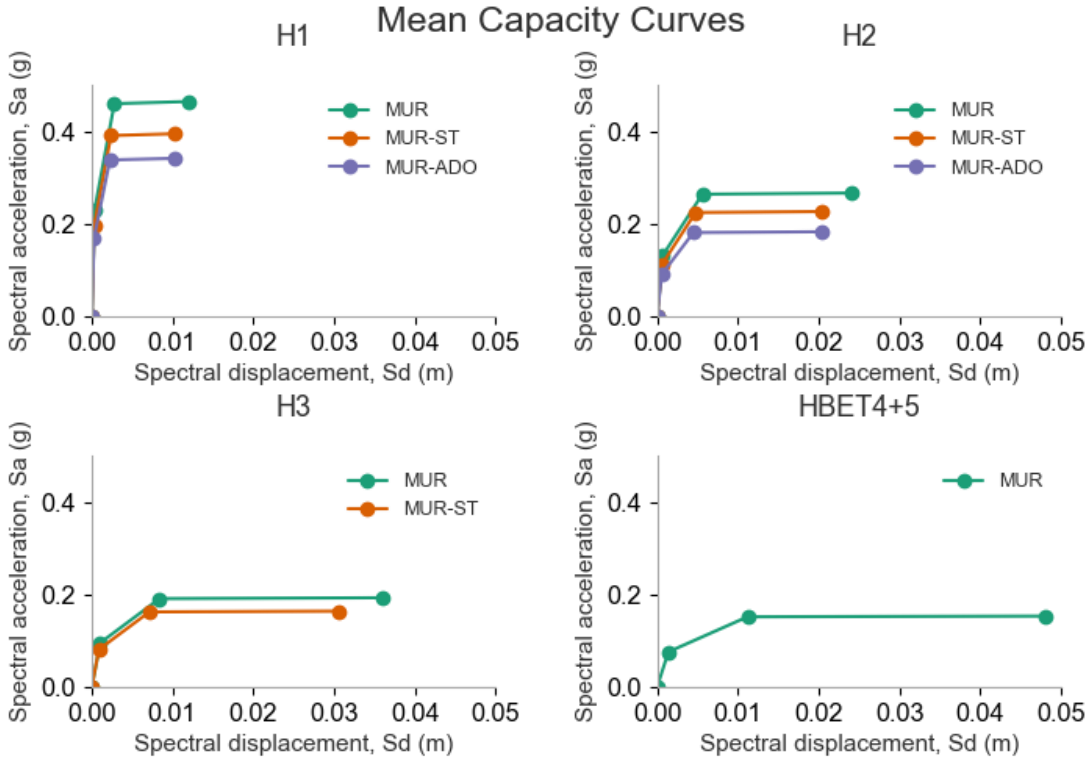

Figure 7: Mean capacity curves for considered building typologies within this case study

Table 6: Key parameters of considered building typologies within this case study

GEM Taxonomy	Yield period (s)	Sd,y (cm)	Sd,u (cm)
MUR/LWAL/DNO/H:1	0.16	0.04	1.2
MUR/LWAL/DNO/H:2	0.29	0.07	2.4
MUR/LWAL/DNO/H:3	0.42	0.11	3.6
MUR/LWAL/DNO/HBET:4-5	0.55	0.14	4.8
MUR+ADO/LWAL/DNO/H:1	0.16	0.03	1.0
MUR+ADO/LWAL/DNO/H:2	0.32	0.06	2.0
MUR+ST/LWAL/DNO/H:1	0.16	0.03	1.0
MUR+ST/LWAL/DNO/H:2	0.29	0.06	2.0
MUR+ST/LWAL/DNO/H:3	0.42	0.09	3.0

For this study, 100 statistically-consistent random samples were generated based on the mean capacity curves and run through the same analysis approach to determine the impact on vulnerability results. Figure 8 shows the distribution of 100 random samples of the capacity curves for one building typology. A multivariate lognormal distribution was assumed around best-estimate input values for the spectral displacement at yield (initiation of damage) and at ultimate (complete failure), using a correlation of 60% and a coefficient of variation of 30% (Silva, et al., 2014a; Silva, et al., 2014b).

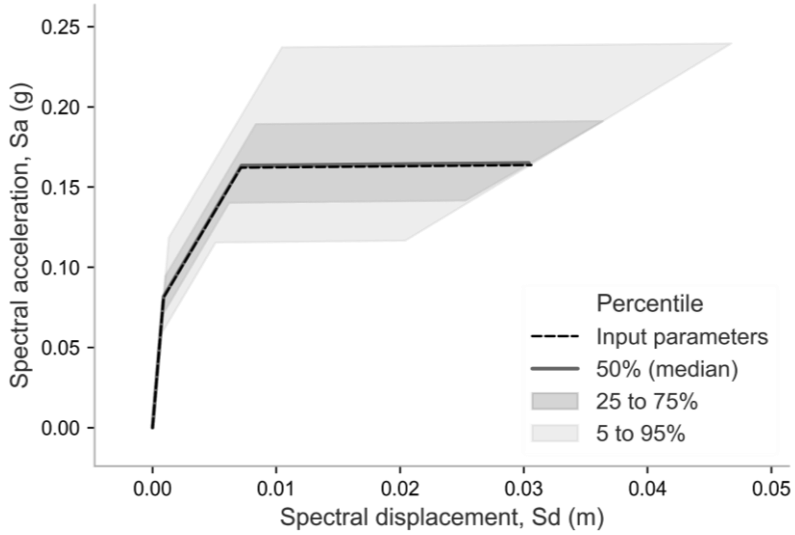

Figure 8: Comparison of resulting capacity curves from 100 random samples of MUR+ST/LWAL+DNO/H:3

The resulting distributions of fragility and vulnerability curves are shown in Figure 9 through Figure 11.

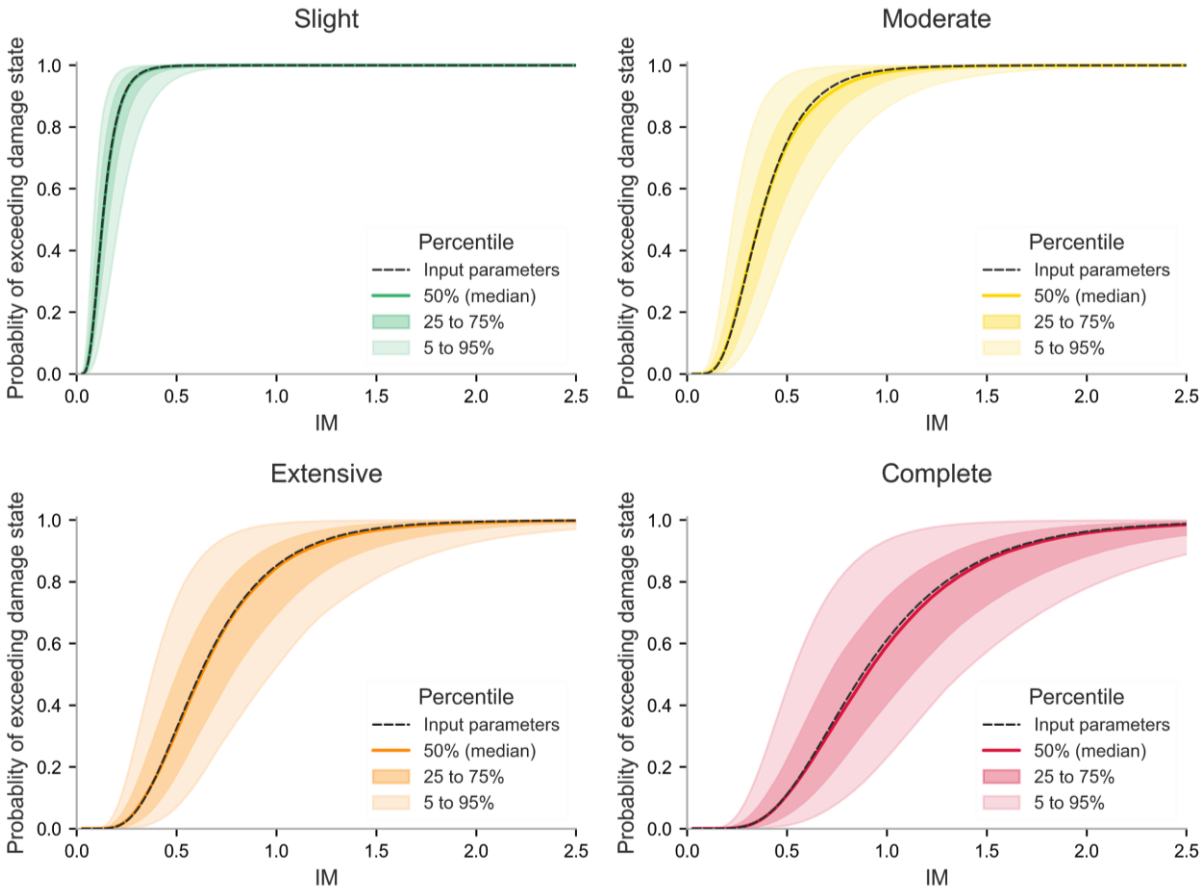

Figure 9: Comparison of resulting fragility curves from random sampling of 100 capacity curves for MUR+ST/LWAL+DNO/H:3

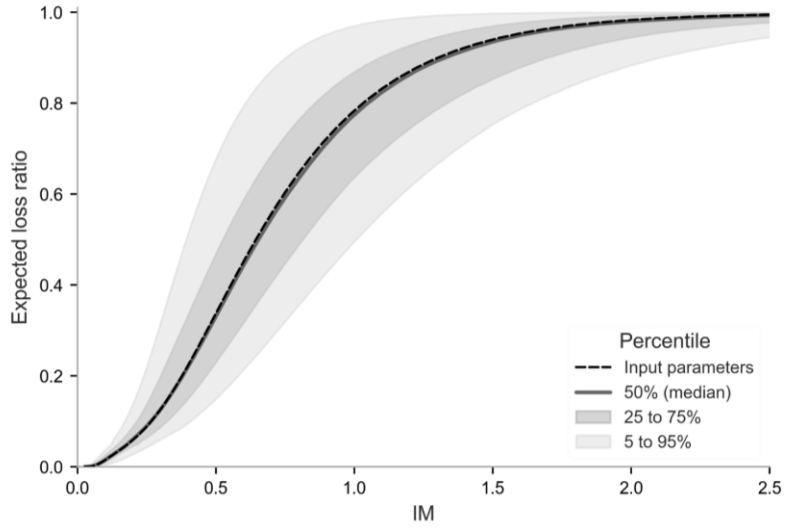

Figure 10: Comparison of resulting vulnerability curves from random sampling of 100 capacity curves for MUR+ST/LWAL+DNO/H:3

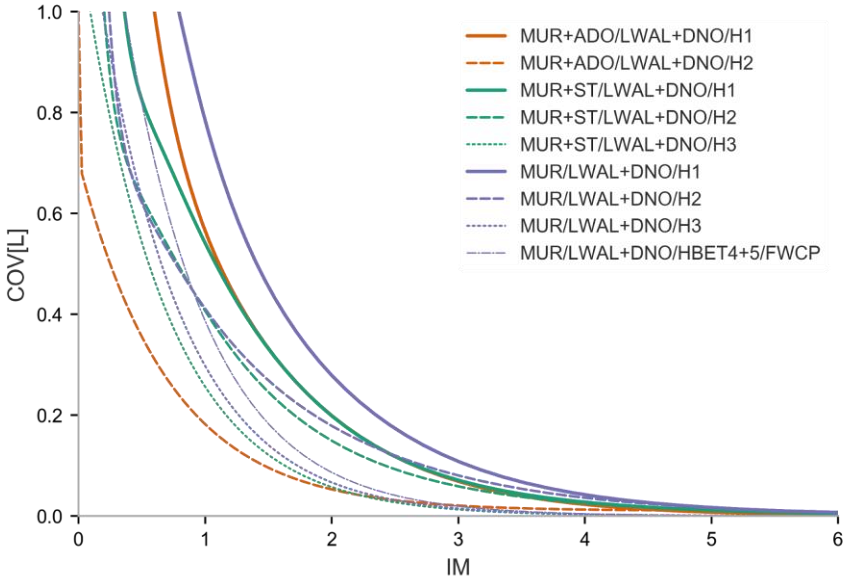

Figure 11: Coefficient of variation of losses for all considered building typologies, by intensity level

While the distribution of derived fragility and vulnerability model outcomes is significant (as evident in Figure 9 to Figure 11), the effect on the range of subsequent risk results is not necessarily as large. To investigate this, each considered building typology was convolved with the hazard curve at a representative site in Nepal to understand the implication on the average annual losses of that building typology. These losses were also converted into an expected loss in 100 years. For reference, the associated hazard curves are presented in Figure 12, which are estimated using the Stevens et. al. model (Stevens, et al., 2018). The impact on disaster risk assessments will be considered further in the forthcoming report (M5.4).

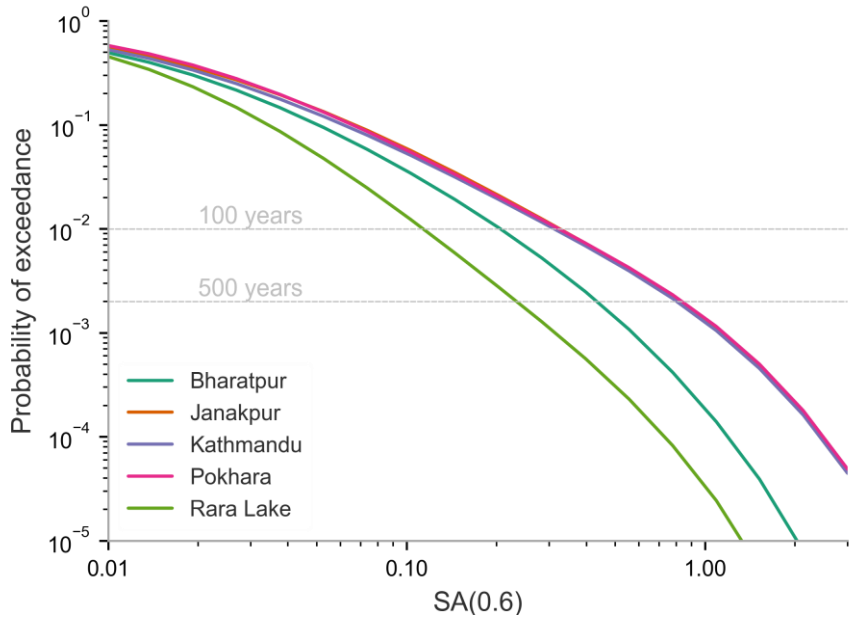

Figure 12: The hazard curves for the considered building typology's intensity measure of interest; Pokhara overlaps with Kathmandu and Janakpur. Estimated using the Stevens et. al. model (Stevens, et al., 2018).

The average annual loss values are summarised in Table 7 for an example building typology. The distribution of average annual losses is shown for all considered building typologies in Figure 13.

Table 7: Average annual loss values for MUR+ST/LWAL+DNO/H:3, considering varying building capacity

Location	5%ile	25%ile	50%ile	75%ile	95%ile
Bharatpur	0.14%	0.23%	0.32%	0.48%	0.74%
Janakpur	0.35%	0.53%	0.71%	0.99%	1.42%
Kathmandu	0.33%	0.49%	0.66%	0.91%	1.31%
Pokhara	0.35%	0.53%	0.70%	0.97%	1.40%
Rara Lake	0.04%	0.07%	0.11%	0.17%	0.28%

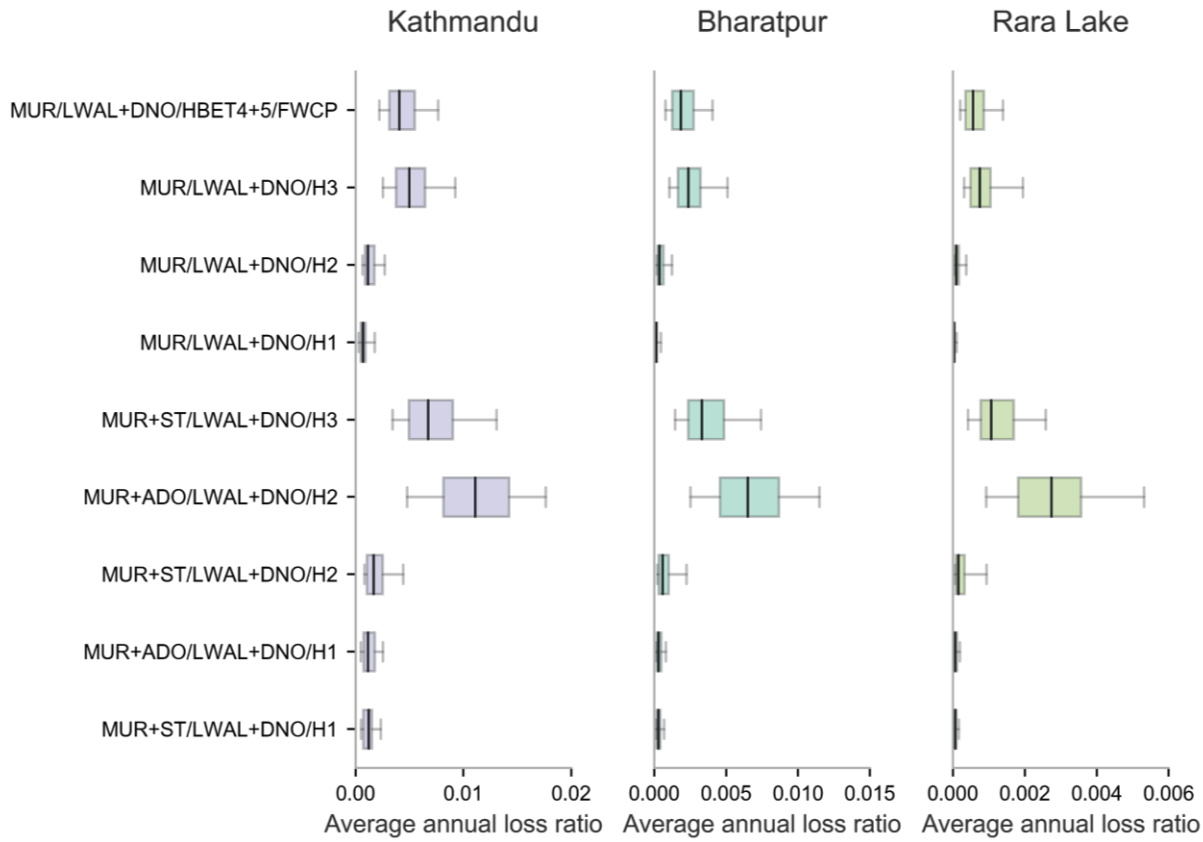

Figure 13: Comparison of percentiles (5%, 25%, 50%, 75%, and 95%) of average annual loss values for Kathmandu and Bharatpur, across all randomly sampled buildings of that typology.

The expected loss in 100 years is shown in Table 8 for all sites, and shown for different timeframes in Kathmandu in Figure 14 and Figure 15.

Table 8: Expected loss in 100 years at different percentiles for MUR+ST/LWAL+DNO/H:3, considering varying building capacity

Location	5%ile	25%ile	50%ile	75%ile	95%ile
Bharatpur	2.9%	4.8%	6.5%	9.5%	15.0%
Janakpur	7.3%	11.2%	16.3%	25.0%	39.0%
Kathmandu	6.8%	10.2%	14.8%	22.8%	35.8%
Pokhara	7.2%	11.0%	16.1%	24.6%	38.5%
Rara Lake	0.7%	1.6%	2.3%	3.4%	5.1%

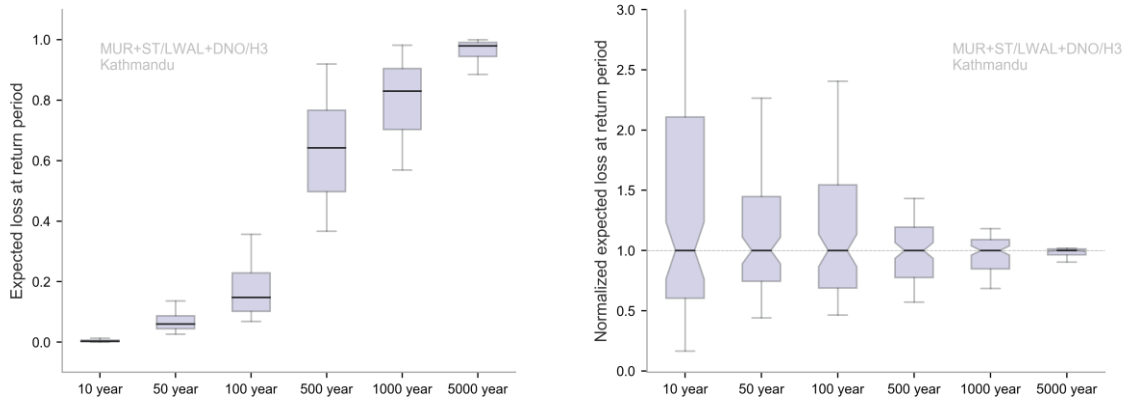

Figure 14: Expected loss in different timeframes for MUR+ST/LWAL+DNO/H:3 at different percentiles (5%, 25%, 50%, 75%, and 95%) in Kathmandu, shown as absolute values (left) and normalized values (right)

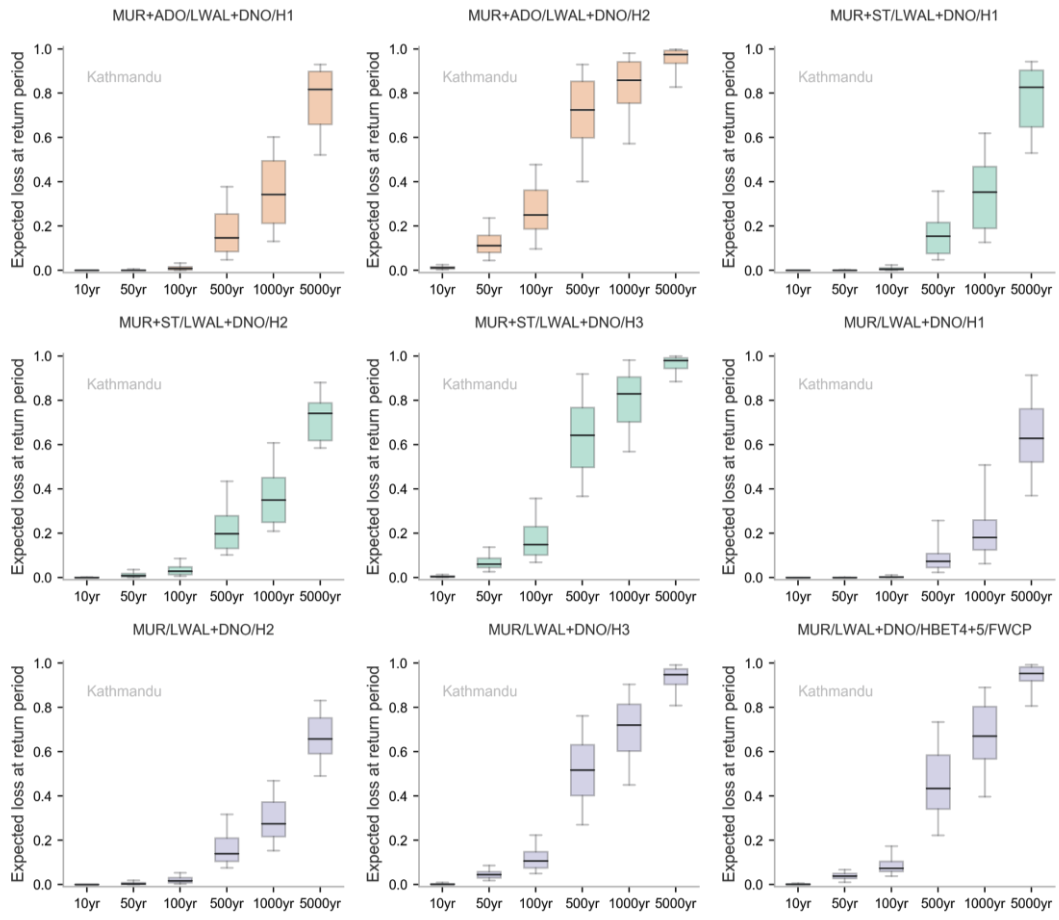

Figure 15: Expected loss in different timeframes for all considered building typologies at different percentiles (5%, 25%, 50%, 75%, and 95%) in Kathmandu

4.4. Damage state variability

The derivation of fragility curves also relies on the identification of different damage states (e.g., slight, moderate, extensive, complete) and the corresponding criteria or thresholds for a building to enter those damage states. However, the determination of these thresholds has both epistemic uncertainty (e.g., how many damage states are chosen) and inherent randomness (e.g., a building may enter 'slight' damage at different levels of response). This uncertainty was incorporated by including additional variability in the demand threshold at which each sequential damage state was entered. An additional dispersion of 0.3 was included (Casotto, et al., 2015; Silva, et al., 2013; FEMA, 2014), which was combined with the best-fit regression dispersion using the SRSS method (i.e., square root of the sum of the squares).

Comparisons of the resulting fragility and vulnerability models derived for an example building typology are shown in Figure 16 and Figure 17, respectively.

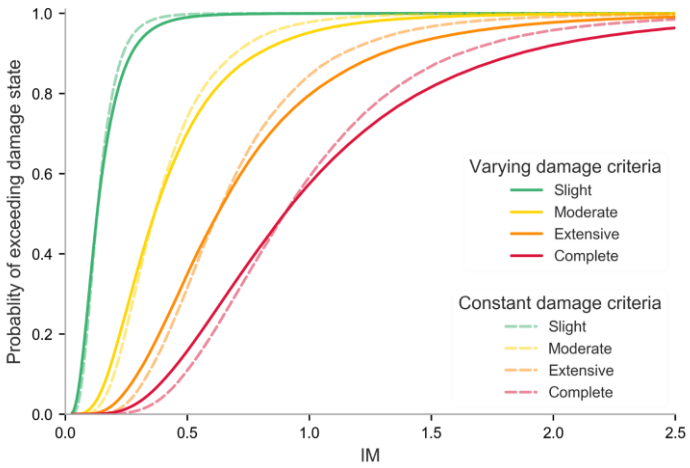

Figure 16: Resulting fragility curves with and without varying damage criteria for MUR+ST/LWAL+DNO/H:3

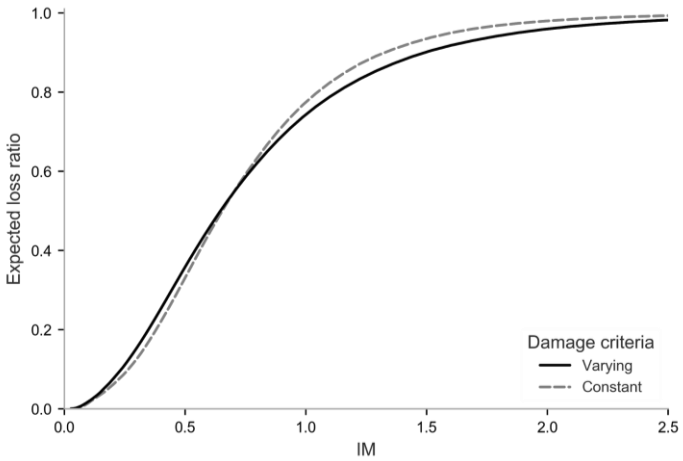

Figure 17: Resulting vulnerability curves with and without varying damage criteria for MUR+ST/LWAL+DNO/H:3

The effect of this additional layer of uncertainty on the expected losses are presented in Table 9 and Table 10. In these results, the additional damage state variability (or demand variability) is included on top of the building capacity variability outlined in the previous section. Percentiles of loss exceedance curves are shown in Figure 18.

Table 9: Average annual losses for MUR+ST/LWAL+DNO/H:3, considering both varying building capacity and varying damage criteria

Location	5%ile	25%ile	50%ile	75%ile	95%ile
Bharatpur	0.17%	0.28%	0.39%	0.58%	0.87%
Janakpur	0.40%	0.61%	0.80%	1.11%	1.59%
Kathmandu	0.37%	0.56%	0.74%	1.02%	1.46%
Pokhara	0.40%	0.60%	0.80%	1.10%	1.57%
Rara Lake	0.05%	0.10%	0.14%	0.22%	0.36%

Table 10: Expected losses in 100 years for MUR+ST/LWAL+DNO/H:3, considering both varying building capacity and varying damage criteria

Location	5%ile	25%ile	50%ile	75%ile	95%ile
Bharatpur	3.5%	5.6%	8.0%	11.7%	18.0%
Janakpur	8.8%	13.5%	19.2%	27.7%	40.8%
Kathmandu	8.1%	12.4%	17.6%	25.6%	38.0%
Pokhara	8.7%	13.3%	19.0%	27.4%	40.4%
Rara Lake	1.0%	2.0%	2.7%	4.1%	6.0%

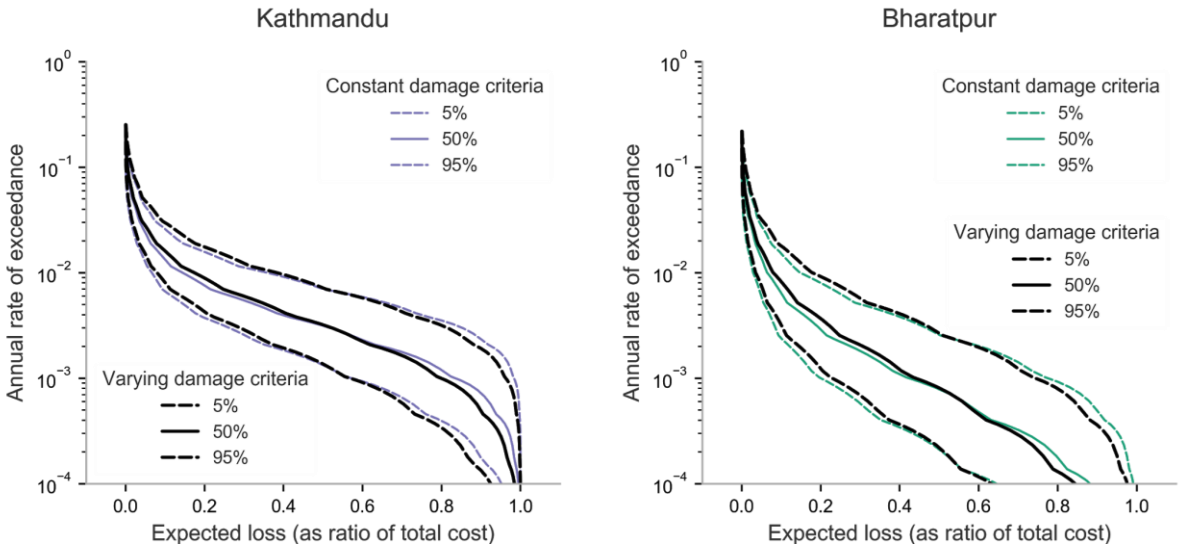

Figure 18: Annual loss exceedance curves for MUR+ST/LWAL+DNO/H:3 in Kathmandu and Bharatpur, with and without varying damage criteria

As seen from the results shown, inclusion of variability in the damage criteria further increases the range of uncertainty. Notably, the values at each percentile tend to shift to be higher (i.e., larger value of loss) for rare return periods, and lower for more frequent return periods. This implies that loss estimates that do not include uncertainty in the damage criteria could be systematically over or underestimated. However, the range of increase is not as substantial as the total uncertainty already included from inclusion of both the hazard input variability and the building capacity variability.

4.5. Loss ratio variability

Damage states are mapped to economic losses in order to construct vulnerability curves and calculate loss estimates (e.g., average annual, probable maximum). The mapping could use expected values (i.e. singular values) for each damage state, or a distribution of losses. This report investigated the impact of either option on the resulting vulnerability models.

Similar to the other areas of uncertainty, damage-based loss ratios have both inherent randomness and epistemic uncertainty. Damage-to-loss models have been proposed using a variety of distribution types (e.g., lognormal, Beta) and underlying data (e.g., insurance claims). For this study, a Beta distribution was investigated, due to further flexibility in its shape to account for concentration of loss ratios close to 0 or 1, as evidenced in some past earthquake events (Silva, 2019; Peiris, et al., 2014; Shome, et al., 2012). The parameters assumed are shown in Table 11, with the corresponding cumulative density functions shown in Figure 19.

Table 11: Assumed Beta distribution parameters for probabilistic loss ratio for each considered damage state

Damage state	Mean	CoV	Alpha	Beta
Slight	0.05	0.3	10.5	199.6
Moderate	0.20	0.2	19.8	79.2
Extensive	0.60	0.1	39.4	26.3
Complete	1.00	0.0	--	--

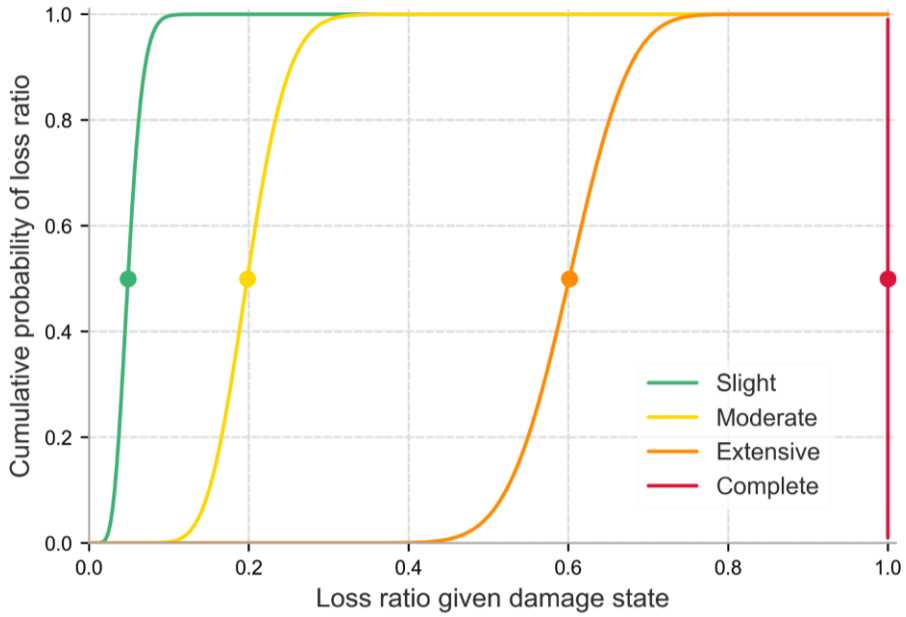

Figure 19: Assumed Beta distributions for probabilistic loss ratio for each considered damage state

The same fragility and vulnerability derivation process was followed using the constant and varying damage-to-loss assumptions, with results shown in Figure 20.

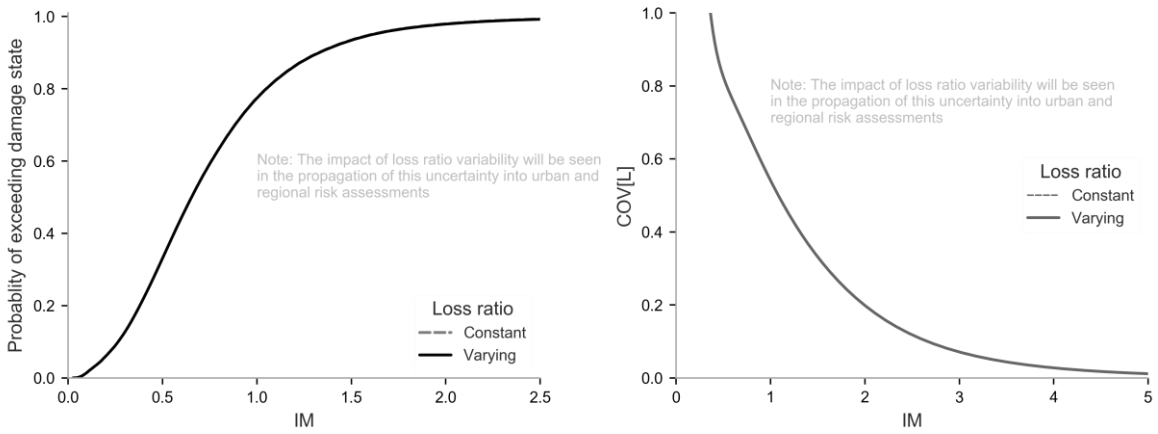

Figure 20: Comparison of resulting vulnerability curve (left) and coefficient of variation of expected loss (right) for varying intensity levels, with and without loss ratio variability for MUR+ST/LWAL+DNO/H:3

While the results in Figure 20 give the illusion that incorporation of uncertainty in the damage-to-loss ratio does not have an impact, further work to propagate the varying damage-to-loss ratios to urban and regional risk assessment will show a difference. This is because this report is limited to investigation on the vulnerability models, which themselves show central (i.e., median) numerical estimates of loss. In an urban or regional assessment, the uncertainty can be included such that different buildings within a spatial area can have differing loss values in a given realisation. Once aggregated across the considered spatial region and number of realisations, a larger distribution of disaster risk loss results is anticipated.

5. Next steps

This report investigated the propagation of uncertainty on vulnerability models, which are used as a component of disaster risk assessment. While this is informative, and considering different aspects of uncertainty has shown to have a significant impact on the derived analytical vulnerability models, the impact on disaster risk assessment results is not yet demonstrated. The next step for this work package is to investigate the propagation of these uncertainties on urban and regional risk assessments. To do so, scenario and fully probabilistic risk assessments will be carried out for the urban area of Kathmandu and the national area of Nepal. The results will be compared across the different cases shown in

Table 12.

Table 12: Considered cases to be compared in forthcoming report, at the urban and regional risk assessment levels

Case	Uncertainty included in...		
	Capacity curve	Damage measure	Loss ratio
1			
2	✓		
3	✓	✓	
4		✓	
5		✓	✓
6			✓
7	✓		✓
8	✓	✓	✓

6. References

Blong, R. J., P. Grasso, S. F. Jenkins, C. R. Magill, T. M. Wilson, K. McMullan and J. Kandlbauer. 2017. "Estimating building vulnerability to volcanic ash fall for insurance and other purposes." *Journal of Applied Volcanology* (1): 1-13.

Casotto, C., V. Silva, H. Crowley, R. Nascimbene and R. Pinho. 2015. "Seismic fragility of Italian RC precast industrial structures." *Engineering Structures* 94: 122-136.

Chandramohan, R., J. Baker and G. Deierlein. 2016. "Quantifying the influence of ground motion duration on structural collapse capacity using spectrally equivalent records." *Earthquake Spectra* 32 (2): 927-950.

Dabbeek, J. and V. Silva. 2020. "Modeling the residential building stock in the Middle East for multi-hazard risk assessment." *Natural Hazards* 100 (2): 781-810.

Elenas, A. and K. Meskouris. 2001. "Correlation study between seismic acceleration parameters and damage indices of structures." *Engineering Structures* 23 (6): 698-704.

FEMA. 2014. *HAZUS-MH MR5, Technical Manual.* Department of Homeland Security - Federal Emergency Management Agency.

Fotopoulou, S.D. and K.D. Pitilakis. 2013. "Fragility Curves for Reinforced Concrete Biuldings to Seismically Triggered Slow-Moving Slides." *Soil Dynamics and Earthquake Engineering* 48: 143-161.

Gehl, P., D. Seyedi and J. Douglas. 2013. "Vector-valued fragility functions for seismic risk evaluation." *Bulletin of Earthquake Engineering* 11 (2): 365-384.

Guillard-Gonçalves, C., J. Zêzere, S. da Silva Pereira and R. A. Garcia. 2016. "Assessment of physical vulnerability of buildings and analysis of landslide risk at the municipal scale: application to the Loures municipality, Portugal." *Natural Hazards and Earth System Sciences* 16 (2): 311-331.

Haugen, E. and A. Kaynia. 2008. *Vulnerability of Structures Impacted by Debris Flow.* London: Taylor & Francis.

Huyck, C., Z. Hu, G. Amyx, M. Esquivias and M. Eguchi. 2019. "Exposure Data Classification, Metadata Population and Confident Assessment." METEOR Report 3.2.

Jenkins, S.F., R. Spence, J.F.B.D. Fonseca, R.U. Solidum and T.M. Wilson. 2014. "Volcanic risk assessment: Quantifying physical vulnerability in the built environment." *Journal of Volcanology and Geothermal Research* 276: 105-120.

Kundzewicz, Z.W., Kanae, S., Seneviratne, S.I., Handmer, J., Nicholls, N., Peduzzi, P., Mechler, R., Bouwer, L.M., Arnell, N.,, Mach, K., Muir-Wood, R. 2014. "Flood risk and climate change: global and regional perspectives." *Hydrological Sciences Journal* 59 (1): 1-28.

Magill, C. and R. Blong. 2005. "Volcanic risk ranking for Auckland, New Zealand. II: Hazard consequences and risk calculation." *Bulletin of Volcanology* 67 (4): 340-349.

Peiris, N., D.A. Gatey and M. Hill. 2014. "Development of a Framework to Model Flood Loss Uncertainty." *Second International Conference on Vulnerability and Risk Analysis and Management (ICVRAM) and the Sixth International Symposium on Uncertainty, Modeling, and Analysis (ISUMA).* Liverpool, UK.

Pomonis, A., R. Spence and P. Baxter. 1999. "Risk assessment of residential buildings for an eurption of Furnas Volcano, São Miguel, the Azores." *Journal of Volcanology and Geothermal Research* 92 (1): 107-131.

Pregnolato, M., C. Galasso and F. Parisi. 2015. "A compendium of existing vulnerability and fragility relationships for flood: preliminary results." *12th International Conference on Applications of Statistics and Probability in Civil Engineering, ICASP12.* Vancouver, BC, Canada.

Shome, N., N. Jayaram and M. Rahnama. 2012. "Uncertainty and Spatial Correlation Models for Earthquake Losses." *15th World Conference on Earthquake Engineering* . Lisbon, Portugal. 24-28.

Silva, V., H. Crowley, R. Pinho and H. Varum. 2013. "Extending displacement-based earthquake loss assessment (DBELA) for the computation of fragility curves." *Engineering Structures* 56: 343-356.

Silva, V., H. Crowley, R. Pinho, H. Varum and R. Sousa. 2014a. "Evaluation of analytical methodologies to derive vulnerability functions." *Earthquake Engineering and Structural Dynamics* 43 (2): 181-204.

Silva, V., H. Crowley, R. Pinho and H. Varum. 2014b. "Investigation of the Charcteristics of Portuguese Regular Moment-frame RC Buildings and Development of a Vulnerability Model." *Bulletin of Earthquake Engineering* 13 (5): 1455-1490.

Silva, Vitor. 2019. "Uncertainty and correlation in seismic vulnerability functions of building classes." *Earthquake Spectra* 35 (4): 1515-1539.

Singh, A., D. P. Kanungo and Shilpa Pal. 2019. "Physical vulnerability assessment of buildings exposed to landslides in India." *Natural Hazards* 96 (2): 753-790.

Sousa, L., V. Silva, M. Marques and H. Crowley. 2015. "Including multiple ground motion intensity measures in the derivation of vulnerability functions for earthquake loss estimation." *SECED Conference: Earthquake Risk and Engineering towards a Resilient World.* 9-10.

Sparks, R.S., W.P. Aspinall, H.S. Crosweller and T.K. Hincks. 2013. "Risk and uncertainty assessment of volcanic hazards." In *Risk and Uncertainty Assessment for Natural Hazards*, 364-398.

Spence, R., J.C. Komorowski, K. Saito, A. Brown, A. Pomonis, G. Toyos and P. Baxter. 2008. "Modelling the impact of a hypothetical sub-Plinian eruption at La Soufrière of Guadeloupe (Lesser Antilles)." *Journal of Volcanology and Geothermal Research* 178 (3): 5160528.

Stevens, V. L., S. N. Shrestha and D. K. Maharjan. 2018. "Probabilistic Seismic Hazard Assessment of Nepal." *Bulletin of the Seismological Society of America* 108 (6): 3488-3510.

Winson, A., J. Crummy, K. Mee, D. Boon, R. Ciurean, C. Dashwood, M. Garcia-Bajo, C. Sampson and V. Silva 2019. METEOR Hazard Footprints for Nepal and Tanzania. METEOR Report M6.1C.

Wilson, G., T.M. Wilson, N.I. Deligne and J.W. Cole. 2014. "Volcanic hazard impacts to critical infrastructure: A review." *Journal of Volcanology and Geothermal Research* 286: 148-182.

Zerger, A., D.I. Smith, G.J. Hunter and S.D. Jones. 2002. "Riding the Storm: A Comparison of Uncertainty Modelling Techniques for Storm Surge Risk Management." *Applied Geography* 22 (3): 307-330.

Zuccaro, G., F. Cacace, R. Spence and P. Baxter. 2008. "Impact of explosive eruption scenarios at Vesuvius." *Journal of Volcanology and Geothermal Research* 178 (3): 416-453.